Ultrafast Double Pulse All-Optical Reswitching of a Ferrimagnet

C. Banerjee, K. Rode, G. Atcheson, S. Lenne, P. Stamenov, J. M. D. Coey, and J. Besbas*
CRANN, AMBER and School of Physics, Trinity College Dublin, Dublin 2, Ireland

(Received 12 December 2020; accepted 22 March 2021; published 27 April 2021)

All-optical reswitching has been investigated in the half-metallic Heusler ferrimagnet $Mn_2Ru_{0.9}Ga$, where Mn atoms occupy two inequivalent sites in the XA-type structure. The effect of a second 200 fs, 800 nm laser pulse that follows the first pump pulse, when both are above the threshold for switching, is studied as a function of t_{12}, the time between them. Aims were to determine the minimum time needed for reswitching and to identify the physical mechanisms involved. The time trajectory of the switching process on a plot of sublattice angular momentum, S^{4a} vs S^{4c}, is in three stages; when $t < 0.1$ ps, the sublattice moments are rapidly disordered, but not destroyed, while conserving net angular momentum via optical spin-wave excitations. This leads to transient parallel alignment of the residual Mn spins in the first quadrant. The net angular momentum associated with the majority sublattice then flips after about 2 ps, and a fully reversed ferrimagnetic state is then established via the spin-lattice interaction, which allows reswitching provided $t_{12} > 10$ ps.

DOI: 10.1103/PhysRevLett.126.177202

Single pulse all-optical switching of magnetization (SP-AOS) is of both fundamental and technological interest [1–3]. Despite intense scrutiny over the last two decades, the microscopic origin of the effect is still poorly understood. However, the possibility of switching the magnetization of a thin film between two stable states on a picosecond timescale without recourse to an external magnetic field is intriguing and technologically relevant in the quest for ever-faster and more energy-efficient information technologies [4–6]. Here we investigate the minimum time that must elapse between two laser pulses, if the second one is to reestablish the original magnetic state after switching by the first pulse [7,8]. Our results advance the fundamental understanding of SP-AOS and highlight its potential for future application in technology.

We have recently shown that the near-cubic XA-ordered ($F\bar{4}3m$) ferrimagnetic Heusler alloy Mn_2Ru_xGa (MRG) exhibits SP-AOS [9], and that switching is driven by antiferromagnetic exchange between the crystallographically inequivalent $4a$ and $4c$ Mn sublattices [10]. The inequivalence is the source of two key properties of MRG. First, the states close to the Fermi level are associated predominantly with one of the two sublattices, which we identified in compounds with $x \approx 0.7$ as $4c$ [11], resulting in half-metallic character. This sublattice dominates the magneto-optic Kerr effect (MOKE) [12]. All MOKE-based measurements shall therefore be understood as reflecting the response of the $4c$ sublattice. Second, due to the hierarchy of the intra- and intersublattice exchange constants, $J_{aa} > -J_{ac} > |J_{cc}|$ [13], the $4c$ sublattice exhibits the higher moment at $T = 0$ K, but its magnitude falls faster with temperature than that of $4a$, so that magnetic compensation occurs at a temperature T_{comp} where the two sublattice magnetizations are equal but opposite in sign [11,14]. We found that SP-AOS is only possible below T_{comp}, when at equilibrium the absolute value of the z projection of the angular momentum of $4c$ manganese exceeds that of $4a$ manganese [9,10].

The MRG sample studied here, $Mn_2Ru_{0.9}Ga$, was grown by dc magnetron cosputtering from Mn_2Ga and Ru targets on MgO (001) single crystal substrates heated to 425 °C, using an ultrahigh vacuum multichamber deposition and characterization tool (Trifolium Dubium, National Access Facility). The film was capped by a 2 nm protective layer of naturally oxidized AlO_x, deposited at room temperature, followed by 8 nm of SiO_2. Biaxial, substrate-induced strain induces a slight tetragonal distortion of the cubic Heusler structure, resulting in perpendicular magnetocrystalline anisotropy of the film [15] and a room-temperature coercivity of 450 mT. The compensation temperature was found to be 413 K from a thermal scan of the remnant magnetization, measured by superconducting quantum interference device magnetometry. Further details on the structural, magnetic, magneto-optic, and magnetotransport properties of MRG can be found elsewhere [11,14–16].

200 fs laser pulses ($\lambda = 800$ nm) were sourced from a mode-locked Ti:sapphire-based laser system. The system was operated in single pulse mode for *ex situ* imaging, whereas for stroboscopic time-resolved magnetization dynamics, the pulse repetition rate was 1 kHz. A portion of the beam was used for second harmonic generation in a β-barium borate crystal creating the probe beam ($\lambda = 400$ nm). Its delay, with respect to a pump beam, was adjusted by a mechanical translation stage. A pair of

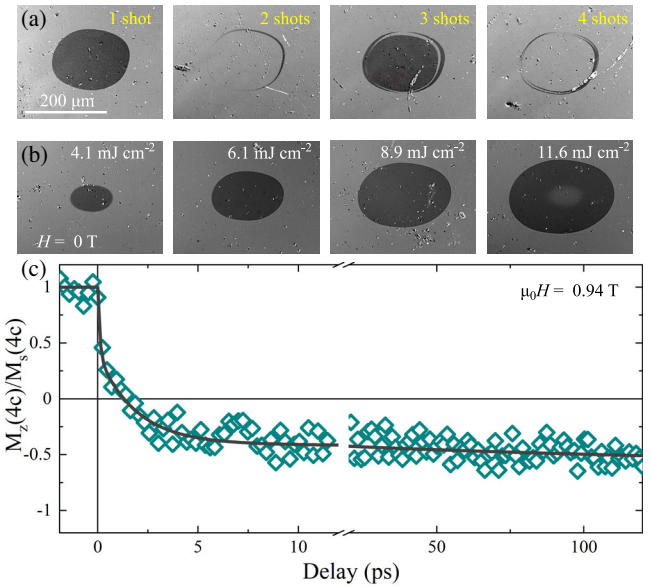

FIG. 1. (a) All-optical toggle switching of magnetization in $Mn_2Ru_{0.9}Ga$ at a fluence of 8.2 mJ cm^{-2}. (b) Domain size as a function of pump fluence. (c) Magnetization dynamics for a pump fluence of 8.9 mJ cm^{-2}. The solid line is a guide to the eye based on three exponentials with characteristic times 100 fs, 1.9 ps, and 320 ps.

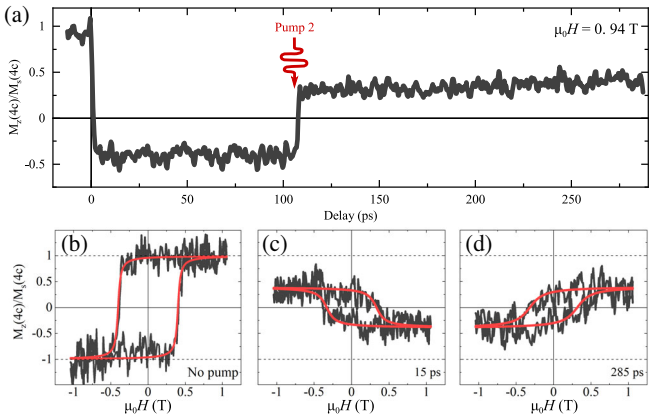

FIG. 2. (a) Transient Kerr signal in presence of two pump pulses separated by 110 ps. (b) Hysteresis loop measured by the probe beam in absence of any pump excitation. (c),(d) Field loops at delays $t_{12} = 15$ ps and 285 ps.

pulses with variable delay were generated from a single pulse using a Michelson interferometer on the pump beam path with one arm mounted on a mechanical translation stage. MOKE imagery was recorded *ex situ* after exposure using an EVICO Kerr microscope with red light in zero applied magnetic field. For all stroboscopic measurements, an applied field of 950 mT was applied perpendicular to the sample surface using an electromagnet.

Figure 1(a) illustrates the toggle nature of SP-AOS. After the first pump exposure, the irradiated spot reverses its magnetization, and subsequent pulses toggle the magnetization back and forth. We also show MOKE micrographs for varying pump fluences [Fig. 1(b)] from which the Gaussian pump beam diameter and the threshold for switching were determined using the Liu method [17]. We find a threshold of 3.5 mJ cm^{-2} and a spot size of about 190 μm.

In Fig. 1(c), we plot the time evolution of the MOKE after a single pump of 8.9 mJ cm^{-2}, well above threshold. The solid guideline is based on three exponentials with characteristic times 100 fs, 1.9 ps and 320 ps. Since our probe pulse has duration ~200 fs, while the pump is slightly stretched to ~250 fs, due to additional optical elements in the beam path, our time resolution is ~325 fs. The two characteristic times are in agreement with our understanding of the SP-AOS process in MRG: Immediately after the pump, the two sublattices demagnetize while conserving net angular momentum such that $dS_z^{4a}/dt = -dS_z^{4c}/dt$ [9,10]. This step is governed by the intersublattice exchange, and it leads to a state where the average z projections of the two sublattice moments are aligned parallel because $|S_z^{4c}| > |S_z^{4a}|$. This is referred to as the transient ferromagneticlike state [1], and it is a necessary but not sufficient condition for switching [18]. The associated timescale is ~150 fs for $Gd(FeCo)_3$ [1] and ~50 fs for MRG because of the ~3 times stronger intersublattice exchange constant in the manganese alloy [13]. We infer that, for times $t \leq 325$ fs, the $4a$ sublattice has switched its orientation, while $4c$ has not. At longer times, $t > 325$ fs, a second process becomes dominant. Angular momentum is no longer conserved, which allows the $4c$ sublattice to switch at $t \sim 1$ ps and a quasistatic state is reached at $t \sim 10$ ps, consistent with the spin-lattice relaxation time in MRG [10]. On a longer timescale of ~300 ps, the lattice cools down to near-ambient temperature by heat flow into the substrate.

Figure 2(a) illustrates the switching with two pump pulses. A first pulse at $t = 0$ reverses the magnetization; a second pulse at $t_{12} = 110$ ps toggles it back. To confirm that magnetic switching actually occurred, we first recorded a MOKE field loop before any excitation [Fig. 2(b)], then one at $t = 15$ ps after a first pump pulse [Fig. 2(c)], and another at $t = 285$ ps, after both [Fig. 2(d)]. The sign reversal of the loops confirms the magnetic switching.

We then determine the minimum value of t_{12} that allows the second pulse to toggle the magnetization. Figure 3(a) shows MOKE micrographs after the sample has been irradiated with two pulses of 4.1 mJ cm^{-2}, separated by $t_{12} = 9$, 11, 11.7, or 12 ps. The first pulse switches the area where the intensity of the Gaussian beam exceeds the threshold at room temperature and also increases the lattice temperature by approximately 65 K in about 2 ps [9]. This increased temperature decays slowly by heat flow to the substrate. As the threshold fluence decreases with increasing temperature (decreasing net magnetization), the second

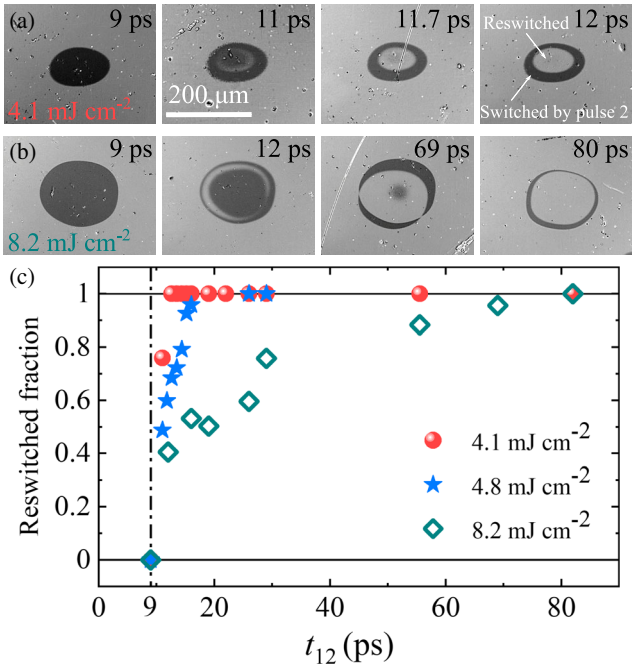

FIG. 3. (a) Kerr micrographs of the irradiated region taken after dual pump excitation for different times t_{12} separating the pulses. Both pump fluences are 4.1 mJ cm^{-2}. For $t_{12} = 12$ ps, the bright center has been switched by the first pulse and toggled by the second, while the surrounding dark ring has been switched by the second pulse as described in the text. (b) Same as (a), but the first and second pump fluences are 8.2 and 6 mJ cm^{-2}, respectively. (c) Variation of the reswitched fraction with t_{12} for first:second pump fluences 4.1:4.1, 4.8:4.8, and 8.2:6.0 mJ cm^{-2}.

pulse toggles an area that is *bigger* than the first. This is clearly visible in Fig. 3(a) for 12 ps pump separation: the central bright spot was switched once by the first pump, then toggled back again by the second, while the dark ring surrounding it is unchanged magnetically by the first and switched by the second. The threshold fluence at this transient higher temperature (365 K) is only 2.9 mJ cm^{-2}, determined from the ratio of the toggled areas.

Reswitching does not occur at a pump separation of 9 ps, whereas at $t_{12} = 12$ ps it is complete. For pump separations of 11.0 and 11.7 ps, we find a third central region where reswitching was not achieved because the higher peak pump intensity requires a longer time to reach equilibrium, even though the relevant time constants are the same. This is illustrated in Fig. 3(b), where we increase the fluence of the first pump to 8.2 mJ cm^{-2} and the second to 6.1 mJ cm^{-2}. For these fluences, the areas switched by the first pump and reswitched by the second are nearly equal, and the central nonreswitching area remains visible up to a pump separation of 70 ps. The results are summarized in Fig. 3(c), where we show the reswitched fraction as a function of pump separation t_{12} for fluences of 4.1, 4.8, and 8.2 mJ cm^{-2}. We highlight two points in the data. First, the lattice temperature does *not* need to exceed T_{comp} to ensure switching, as observed in $Gd(FeCo)_3$—excessive heating actually prevents reswitching. Second, the fundamental limit on repetition rate is not uniquely determined by the heat transfer to the substrate. The relevant time is the spin-lattice relaxation time: the time needed for magnetic damping.

Based on the original studies of amorphous $Gd(FeCo)_3$ [1,2], SP-AOS was believed to depend on two conditions. First, it was thought that the demagnetization times of the two sublattices needed to be substantially different, so that the z projections of their moments could cross zero at different times. Second, it was thought that high-spin polarization inhibited efficient demagnetization. These expectations were overturned by our observation of switching in MRG. There, unlike $Gd(FeCo)_3$, the two sublattices composed of the same element would be expected to demagnetize at similar rates. Furthermore, although one of the sublattices contributes the overwhelming majority of the states at the Fermi level, the material nevertheless exhibits SP-AOS. We now discuss the situation in light of our new findings.

The on-atom Coulomb interaction integrals for $3d^5$ manganese (Slater F^2 and F^4) are 0.6 and 0.4 Ry (8.2 and 5.4 eV) and the first thermally excited configuration is $(5/7\text{-}25/49)F^2 + (5/7\text{-}190/441)F^4$ higher in energy, corresponding to an energy of 3.2 eV [19,20]. For MRG we infer that the atomic moment and the exchange integrals remain, to a very good approximation, time independent. The corresponding energies for Gd ($4f^7$), Tb ($4f^9$), Co ($3d^7$), and Fe ($3d^6$) are 3.5, 0.35, 0.14, and 0.07 eV, respectively, suggesting that this will not be the case for Tb, Co, and Fe [21]. Exchange will dominate relaxation in MRG throughout. Iron, on the other hand, only recovers its normal atomic configuration and resumes interatomic exchange with Gd after about 1 ps. Optically induced transitions to excited states do not change the spin due to the magneto-optical selection rules [19]. We must therefore discuss our findings in the language of spin waves and precession [22], noting, however, that the usual models for spin waves assume that the x and y projections of the atomic moments are small ($S_z \gg S_x, S_y$), an assumption that is clearly invalid for SP-AOS.

Ferrimagnets exhibit at least two orthogonal spin-wave modes if axial symmetry is unbroken. In one mode, the two sublattices precess together without changing the angle between them; in the other, they precess in antiphase. The two are frequently referred to as the acoustic or ferromagnetic and optical or antiferromagnetic modes, respectively. In amorphous $Gd(FeCo)_3$, axial symmetry is broken by structural inhomogeneity [22], whereas in MRG noncollinearity of the ferrimagnetic ground state [23], fourfold sublattice-specific magnetocrystalline anisotropy of opposite signs [24], and preferential absorption by light of one sublattice play the same role. The intense electronic excitation provided by the pump pulse excites a multitude of

magnons. In the absence of axial symmetry, the optical mode can be efficiently excited [25], leading to the first-quadrant ferromagnetic aligned state discussed earlier. The relevant times are those associated with interatomic exchange energies via the uncertainty principle ~100 fs, which are comparable to the 200 fs duration of the pulse in our experiments [26]. We note that this process is fast because it conserves angular momentum. It only depends on the magnetic system absorbing the energy deposited by the pump. This is often called exchange scattering [27]. Thermodynamically, the maximum energy that can be absorbed by the magnetic system while conserving angular momentum leads to $S^{4c}_{z\min} = (n_{aa} + n_{ac})/(n_{aa} + n_{cc} + 2n_{ac})(S^{4a}_{z0} + S^{4c}_{z0})$, where n ($n_{ij} > 0$) are the Weiss molecular field constants. S^{4c}_z remains positive, while S^{4a}_z has switched and the associated time is that needed for the first stage of switching.

Following this, the magnetic system loses energy by coupling to the lattice and the $4c$ sublattice reverses its magnetic polarity, the $4a$ sublattice, which has already changed polarity, is increasing. When $4c$ crosses zero, the intersublattice exchange will align it antiparallel to $4a$. This process does not conserve net angular momentum and probably requires emission of optical phonons. The experimentally determined timescale is 1.9 ps, which represents the time needed for the second stage, as both sublattices are now antiparallel to their initial directions. We believe this second stage is driven by continued demagnetization of the $4c$ sublattice. It is telling that the threshold for switching decreases when the temperature increases toward T_{comp}, as the residual z projection at $t = 325$ fs is reduced. We speculate that very close to T_{comp} the threshold fluence for SP-AOS could be very substantially reduced, albeit only for extremely short pump pulses [10].

Lastly, the optical magnons scatter into the long wavelength acoustic modes of frequency ~100 GHz [26] and are damped on the spin-lattice relaxation timescale (~10 ps) when S^{4c}_z regains a higher magnitude than S^{4a}_z, unless the lattice has already heated above T_{comp}. This is the time that finally marks the completion of the magnetic reversal, and it then becomes possible to repeat the process and toggle the magnetization with a second pulse. The half metallicity of MRG is beneficial, as it will increase the damping of the $4c$ sublattice due to Fermi surface breathing [28] and allow it to relax faster than $4a$, decreasing the time that must elapse between subsequent toggle events. The whole three-stage process is illustrated in Fig. 4 by the track from initial to final states, where the relevant times after the pump are marked on a logarithmic scale on the red trajectory. Plausible spin configurations at different times are illustrated in the inset. The four-quadrant representation of a two-sublattice magnet in Fig. 4 that has been used by Mentink *et al.* [29], was originally inspired by Bar'yakhtar [27].

Finally, we comment on the energy requirements for a potential application. We have shown that threshold

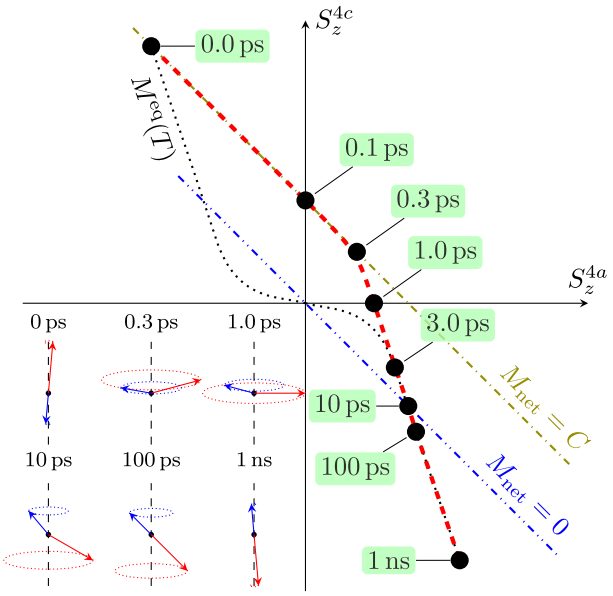

FIG. 4. Magnetization of the $4a$ and $4c$ sublattices during SP-AOS trajectory (red dashed line). The first stage of exchange driven demagnetization switches the $4a$ sublattice while keeping the net magnetization constant; a transient ferromagneticlike state is reached between 0.1 and 0.3 ps. In the second stage, between 0.3 and 3.0 ps, the $4c$ sublattice reverses and the system relaxes toward equilibrium on the black dotted line. Between 3 ps and 1 ns, the system cools down. At 10 ps, the net magnetization changes sign and the system can be than be reswitched. The inset in the third quadrant illustrates the proposed spin configurations.

fluences as low as 2.9 mJ cm^{-2} or 0.3 fJ, suffice to switch a $(10\text{ nm})^3$ element, assuming that 35% of the light is absorbed by a 30 nm thick MRG thin film. This is an order of magnitude more than current records for transparent magnetic insulators [3]. However, the metallic nature of MRG permits integration with other spin electronic circuitry, thereby creating an opportunity to bring the speed of optics to magnetism and electronics. Possible applications include beam steering using diffraction elements, such as Fresnel zone plates, where MRG (or some future material) forms the "dark" elements. The focal point of the zone plate could thus be changed every 10 ps.

In conclusion, the relevant timescales for SP-AOS are the exchange time and the spin-lattice relaxation time, which we evaluate from our two-pulse experiments. We infer that SP-AOS requires axial symmetry breaking, either by structural inhomogeneity or by competition between magnetocrystalline anisotropy and exchange. The hierarchy of exchange constants in a ferrimagnet is critical to promote low-energy SP-AOS. Repeated toggle switching is envisaged at rates as high as 100 GHz, provided the lattice temperature remains below T_{comp}. Reducing the spin-lattice relaxation time could increase this frequency. To our knowledge, this 10 ps result marks the fastest switch yet from one stable magnetic state to another.

This work was supported by Science Foundation Ireland under contract 16/IA/4534 ZEMS and the European Union Horizon 2020 Research and Innovation Grant Agreement No. 737038 TRANSPIRE. C. B. is grateful for support from an Irish Research Council Fellowship. The Trifolium Dubium deposition-characterization platform was funded by Science Foundation Ireland under Grant No. 15/RI/3218. The work was carried out in the CRANN Photonics Laboratory, where we thank Dr. Jing Jing Wang for technical support.

*besbasj@tcd.ie

[1] I. Radu, K. Vahaplar, C. Stamm, T. Kachel, N. Pontius, H. A. Dürr, T. A. Ostler, J. Barker, R. F. L. Evans, R. W. Chantrell, A. Tsukamoto, A. Itoh, A. Kirilyuk, Th. Rasing, and A. V. Kimel, Nature (London) **472**, 205 (2011).
[2] T. A. Ostler *et al.*, Nat. Commun. **3**, 666 (2012).
[3] A. Stupakiewicz, K. Szerenos, D. Afanasiev, A. Kirilyuk, and A. V. Kimel, Nature (London) **542**, 71 (2017).
[4] S. Mangin, M. Gottwald, C.-H. Lambert, D. Steil, V. Uhlíř, L. Pang, M. Hehn, S. Alebrand, M. Cinchetti, G. Malinowski, Y. Fainman, M. Aeschlimann, and E. E. Fullerton, Nat. Mater. **13**, 286 (2014).
[5] C.-H. Lambert, S. Mangin, B. S. D. Ch. S. Varaprasad, Y. K. Takahashi, M. Hehn, M. Cinchetti, G. Malinowski, K. Hono, Y. Fainman, M. Aeschlimann, and E. E. Fullerton, Science **345**, 1337 (2014).
[6] S. Iihama, Y. Xu, M. Deb, G. Malinowski, M. Hehn, J. Gorchon, E. E. Fullerton, and S. Mangin, Adv. Mater. **30**, 1804004 (2018).
[7] K. Szerenos, A. V. Kimel, A. Maziewski, A. Kirilyuk, and A. Stupakiewicz, Phys. Rev. Applied **12**, 044057 (2019).
[8] S. Wang, C. Wei, Y. Feng, H. Cao, W. Li, Y. Cao, B.-O. Guan, A. Tsukamoto, A. Kirilyuk, A. V. Kimel, and X. Li, Light Sci. Appl. **10**, 8 (2021).
[9] C. Banerjee, N. Teichert, K. E. Siewierska, Z. Gercsi, G. Y. P. Atcheson, P. Stamenov, K. Rode, J. M. D. Coey, and J. Besbas, Nat. Commun. **11**, 4444 (2020).
[10] C. S. Davies, G. Bonfiglio, K. Rode, J. Besbas, C. Banerjee, P. Stamenov, J. M. D. Coey, A. V. Kimel, and A. Kirilyuk, Phys. Rev. Research **2**, 032044(R) (2020).
[11] D. Betto, N. Thiyagarajah, Y.-C. Lau, C. Piamonteze, M.-A. Arrio, P. Stamenov, J. M. D. Coey, and K. Rode, Phys. Rev. B **91**, 094410 (2015).
[12] K. Fleisher, N. Thiyagarajah, Y.-C. Lau, D. Betto, K. Borisov, C. C. Smith, I. V. Shvets, J. M. D. Coey, and K. Rode, Phys. Rev. B **98**, 134445 (2018).
[13] C. Fowley, K. Rode, Y.-C. Lau, N. Thiyagarajah, D. Betto, K. Borisov, G. Atcheson, E. Kampert, Z. Wang, Y. Yuan, S. Zhou, J. Lindner, P. Stamenov, J. M. D. Coey, and A. M. Deac, Phys. Rev. B **98**, 220406(R) (2018).
[14] H. Kurt, K. Rode, P. Stamenov, M. Venkatesan, Y.-C. Lau, E. Fonda, and J. M. D. Coey, Phys. Rev. Lett. **112**, 027201 (2014).
[15] N. Thiyagarajah, Y.-C. Lau, D. Betto, K. Borisov, J. M. D. Coey, P. Stamenov, and K. Rode, Appl. Phys. Lett. **106**, 122402 (2015).
[16] N. Teichert, G. Atcheson, K. Siewierska, M. N. Sanz-Ortiz, M. Venkatesan, K. Rode, S. Felton, P. Stamenov, and J. M. D. Coey, Phys. Rev. Materials **5**, 034408 (2021).
[17] J. M. Liu, Opt. Lett. **7**, 196 (1982).
[18] V. N. Gridnev, Phys. Rev. B **98**, 014427 (2018).
[19] R. D. Cowan, *The Theory of Atomic Structures and Spectra* (University of California Press, Berkeley, CA, 1981).
[20] We consider on-atom direct Coulomb interaction and spin-orbit coupling only. We speculate that new materials exhibiting SP-AOS are likely to contain half filled *d* or *f* shells.
[21] B. Koopmans, M. van Kampen, J. T. Kohlhepp, and W. J. M. de Jonge, Phys. Rev. Lett. **85**, 844 (2000).
[22] J. Barker, U. Atxitia, T. A. Ostler, O. Hovorka, O. Chubykalo-Fesenko, and R. W. Chantrell, Sci. Rep. **3**, 3262 (2013).
[23] K. E. Siewierska, G. Atcheson, A. Jha, K. Esien, R. Smith, S. Lenne, N. Teichert, J. O'Brien, J. M. D. Coey, P. Stamenov, and K. Rode, arXiv:2012.05736.
[24] S. Lenne, Y.-C. Lau, A. Jha, G. Y. P. Atcheson, R. E. Troncoso, A. Brataas, J. M. D. Coey, P. Stamenov, and K. Rode, arXiv:1903.04432.
[25] A. Kamra, U. Agrawal, and W. Belzig, Phys. Rev. B **96**, 020411(R) (2017).
[26] G. Bonfiglio, K. Rode, G. Y. P. Atcheson, P. Stamenov, J. M. D. Coey, A. V. Kimel, Th. Rasing, and A. Kirilyuk, J. Phys.: Condens. Matter **33**, 135804 (2021).
[27] V. G. Bar'yakhtar, Zh. Eksp. Teor. Fiz. **87**, 1501 (1984) [J. Exp. Theor. Phys. **60**, 863 (1984)].
[28] V. Kamberský, Czech. J. Phys. **26**, 1366 (1976).
[29] J. H. Mentink, J. Hellsvik, D. V. Afanasiev, B. A. Ivanov, A. Kirilyuk, A. V. Kimel, O. Eriksson, M. I. Katsnelson, and Th. Rasing, Phys. Rev. Lett. **108**, 057202 (2012).